DYNAMIC POWER SPECTRAL ANALYSIS OF SOLAR MEASUREMENTS FROM PHOTOSPHERIC, CHROMOSPHERIC, AND CORONAL SOURCES

S.D. Bouwer, J. Pap, R.F. Donnelly

CIRES, University of Colorado / NOAA, Space Environment Laboratory
Mail code R/E/SE, 325 Broadway, Boulder CO 80303, USA

ABSTRACT

An important aspect in the power spectral analysis of solar variability is the quasistationary and quasiperiodic nature of solar periodicities. In other words, the frequency, phase, and amplitude of solar periodicities vary on time scales ranging from active region lifetimes to solar cycle time scales. In this study we employ a dynamic, or running, power spectral density analysis to determine many periodicities and their time-varying nature in the projected area of active sunspot groups (S_{act}) , the SMM/ACRIM total solar irradiance (S) , the Nimbus-7 MgII center-to-wing ratio ($R(\mathrm{MgII}_{c/w})$) , the Ottawa 10.7 cm flux ($F_{10.7}$) , and the GOES background X-ray flux (X_b) for the maximum, descending, and minimum portions of solar cycle 21 (i.e., 1980–1986). This technique dramatically illustrates several previously unrecognized periodicities. For example, a relatively stable period at about 51 days has been found in those indices which are related to emerging magnetic fields. The majority of solar periodicities, particularly around 27, 150 and 300 days, are quasiperiodic because they vary in amplitude and frequency throughout the solar cycle. Finally, it is shown that there are clear differences between the power spectral densities of solar measurements from photospheric, chromospheric, and coronal sources.

INTRODUCTION

A frequently overlooked aspect in the time series analysis of solar data is that the data are not stationary. A process is generally considered nonstationary if the mean and autocorrelation suddenly changes over time. Bouwer[1] has shown that nonstationarity is particularly true of coronal measurements. As active regions emerge and decay, they generally persist with strong emissions for as long as eight solar rotations. Donnelly *et al.*[2,3] have shown that chromospheric emissions persist longer than coronal emissions. The formation of active regions may occur at different solar latitudes and longitudes which affect both the observed phases and rotation rates. At best, solar time series can be considered quasistationary; i.e., the mean and autocorrelation are either slowly varying, or suddenly changing at the beginning of a new episode of major active region development and remaining relatively constant for the lifetime of the active region complex. The net result in solar time series measurements of these non-random, sudden changes in the frequency and amplitude of solar periodicities is a quasiperiodic time series, i.e., apparent periodicities whose amplitudes come and go over active region lifetimes, and which are modulated in frequency.

The emphasis here in the power spectral analysis is on the quasiperiodic nature of solar variations; consequently we employ a running power spectral density analysis discussed by Bath[4], referred to here simply as a dynamic power spectra. By moving a power spectral density transform through the autocorrelation of the time series data, we illustrate the time-varying characteristics of photospheric, chromospheric, and coronal periodicities on short and intermediate time scales from about twelve days to about a year.

In an analysis technique introduced by Lean and Repoff[5], the basic power spectrum employed here is done without interpolating the original data . Briefly, the power spectrum is calculated by first detrending the time series using an n^{th} – order polynomial to remove the solar cycle. Next the autocorrelation is calculated, tapering the tail of the autocorrelated data to remove spurious sidelobes. The tapering is done in this analysis using a Tukey-Hanning window (a cosine weighing function) starting at lag 205 days. The power spectral density is then calculated by performing a fast Fourier transform on the autocorrelated data. In the figures that follow, the power spectrum is reported as the percent of total power at each frequency.

A dynamic power spectra of solar time series data is calculated here by computing the power spectral density for a relatively short time window (e.g., 1024 days), then successively stepping the window through time (e.g., 27 days) on the autocorrelated data. By then contouring the power found as a function of frequency and time using a triangulation algorithm, an overall picture of how the power spectral density changes over time can be clearly visualized. Because this form of spectral analysis is exploratory, i.e., looking for overall patterns in solar variability, estimates of statistical significance are not calculated. Test cases of known spectral characteristics were used to confirm the overall correctness of the analysis procedures, determine noise estimates, and to find the approximate temporal resolution of the running transform. The running transform is capable of detecting a change in frequency or amplitude within a lag of about 250 days, depending on the relative amplitude of the change. Since an 4^{th} – order polynomial is used to detrend the data for the solar cycle variations and because of the relatively short time windows used in the Fourier transforms, periods in excess of 256 days are not well determined. Furthermore, because the frequency resolution of a Fourier transform is determined by the length of the time series, the frequency resolution at short-term periods (i.e., 16 to 48 days) corresponds to slightly less than a one day difference in period.

Photospheric solar variability is represented in this study with both S and S_{act} , although Smith and Gottlieb[6] have shown that roughly one-third the total solar irradiance variation comes from UV sources primarily chromospheric in origin, and the majority of the remainder from photospheric sources. Projected areas of active sunspot groups, which are defined by Pap[7] as being associated with emerging magnetic fields and are classified as newly formed and developing sunspot groups with gamma or delta magnetic configurations, are considered a better photospheric index than S in this study.

Chromospheric solar variability is represented here using $R(\mathrm{MgII}_{c/w})$. Based on Nimbus-7 satellite UV measurements, the $R(\mathrm{MgII}_{c/w})$ index was developed by Heath and Schlesinger[8] as a relative photometric measure, and as a result it is relatively insensitive to long-term instrumental degradation problems. Tobiska and Bouwer[9] demonstrate that $F_{10.7}$ shows both chromospheric and coronal components in its total flux. Wagner[10] presents X_b flux that represents coronal sources above 3×10^6 °K, where the sources come from the closed magnetic flux loops associated with active regions. All data reported here are from a terrestrial viewpoint (resulting in synodic rotation rates) at one astronomical unit (AU).

RESULTS

In Figure 1 we show the five measurements representing: (1) The hot corona using a background X-ray index (i.e., effects of flares are reduced). (2) A combination of the chromosphere, transition region, and corona using the Ottawa 10.7 cm flux $F_{10.7}$, (3) Chromospheric flux using the Nimbus-

7 UV index $R(\mathrm{MgII}_{c/w})$, (4) Mostly photospheric irradiance using SMM/ACRIM total irradiance S . and (5) Emerging magnetic flux using the projected area of active sunspots S_{act} .

Also shown in the Figure 1 time series as a dashed line is the 4^{th} – order polynomial used to remove the long-term solar cycle variation before calculating the power spectrum. To a first-order approximation, the five time series show similar solar cycle and intermediate-term characteristics. Most important are the intermediate-term variations; all the time series show major episodes of active region evolution lasting about 6-12 solar rotations that have nearly concurrent local minima, particularly during 1981 to 1984. However, the relative persistence of active regions and solar rotational effects differ significantly between the time series, and since the amplitude of these variations are generally about as large as the intermediate variations, a new analysis that accounts for the quasiperiodic nature of the time series is needed to meaningfully distinguish the differences.

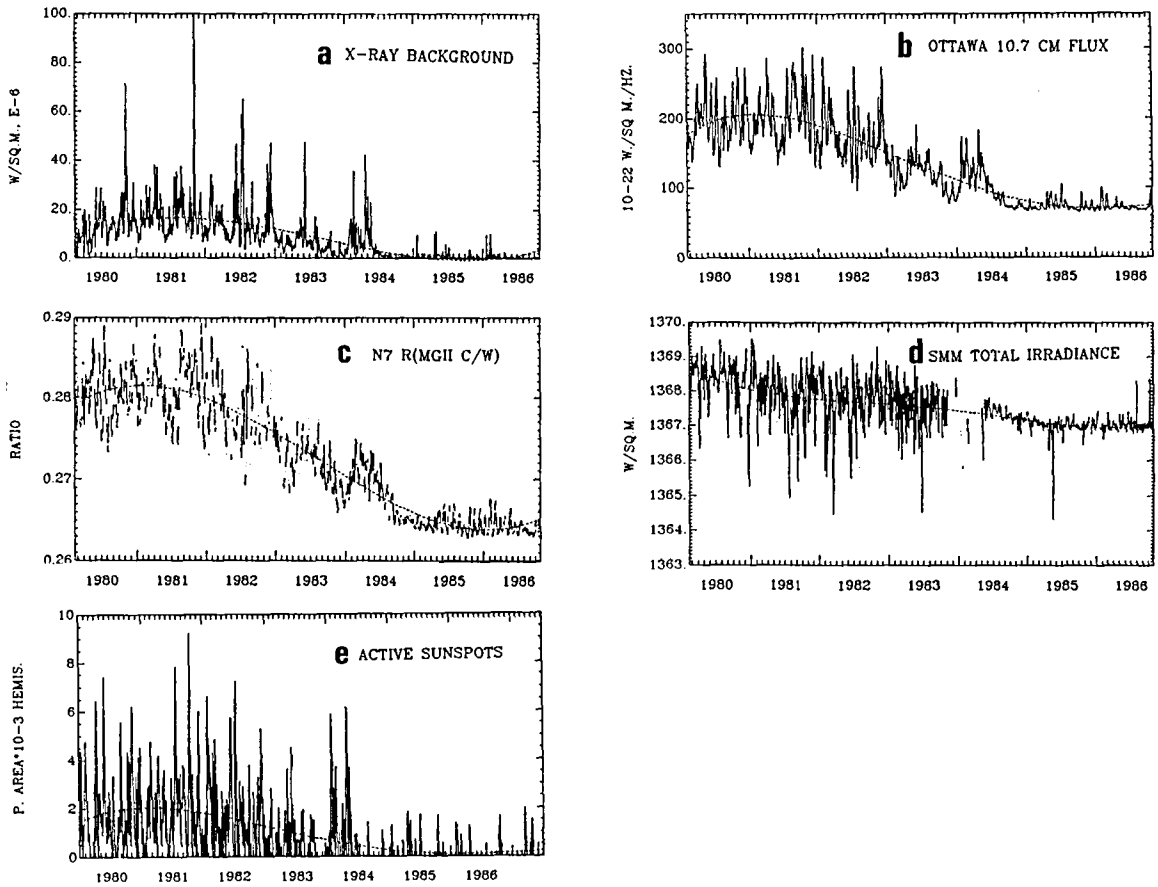

Figure 1. Time series from: (a) GOES Background flux X_b , representing coronal sources, (b) Ottawa 10.7 cm flux $F_{10.7}$ representing both chromospheric and coronal sources (c) Nimbus-7 $R(\mathrm{MgII}_{c/w})$ representing chromospheric sources, (d) SMM Total solar irradiance S representing mostly photospheric sources, and (e) Projected area of active sunspots Sa , representing emerging magnetic fields. All time series are from a terrestrial viewpoint at 1 AU. Also shown as a dashed line is the 4^{th} – order polynomial used to detrend the time series in the subsequent spectral analysis.

The dynamic power spectra calculated from the time series in Figure 1 are shown in Figure 2 as contour diagrams. As the transform is stepped through the autocorrelated data, the date at the center of the transform is calculated and displayed on the left axis. The ordinate is shortened to the length of the time series in which the running transform can detect a change. The synodic

period in days is shown on the bottom axis, and the equivalent frequency in microhertz is shown on the top axis. Each horizontal slice represents a simple power spectrum of power as a function of frequency. In effect, each plot of power as a function of time and frequency is visually much like the elevation data of a mountainous contour map. The highest "peaks" of the mountains in Figure 2 have been truncated by about 0.5% (except S, which was truncated 0.3% from the maximum) below the maximum to make the figure more readable by highlighting the peaks. It is important to note that much of the fine details in the contour diagrams are due to the combined effects of "noisy" data and the limitations of the power spectral analysis and contouring algorithm. Nevertheless, the overall patterns are accurate and are the important results of this study.

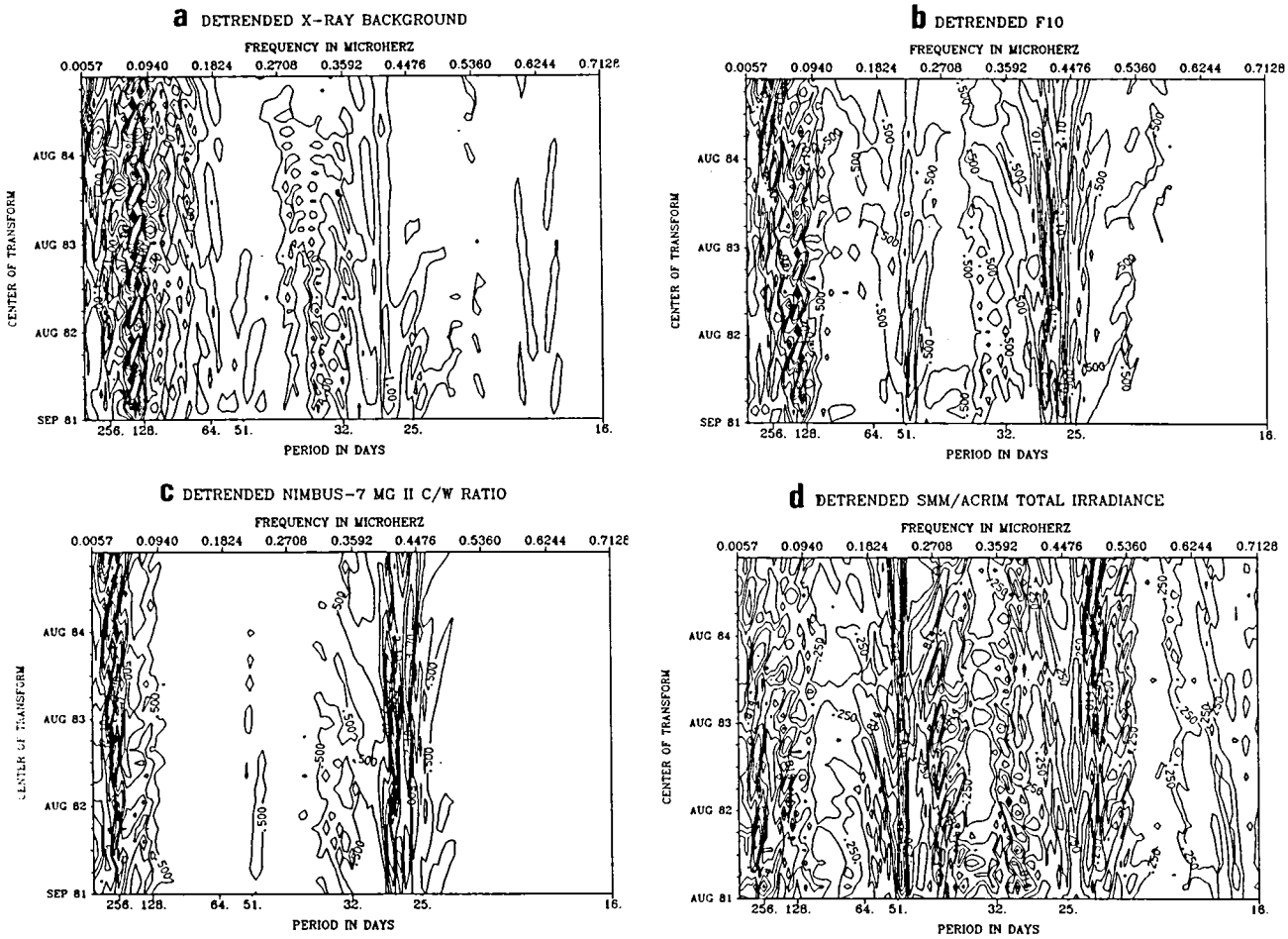

Figure 2. Dynamic power spectra of: (a) Background X-ray X_b , (b) Ottawa 10.7 cm flux $F_{10.7}$, (c) Nimbus-7 $R(\mathrm{MgII}_{c/w})$, and the SMM total solar irradiance S . The ordinate shows the center date of the running time window, which can detect a change in the time series to within about a 250-day lag. Power is indicated as the percent of total power, and spectral noise is estimated to be 0.25% of total power. For (a), the contour lines start at 0.50 and proceed to a 4.1 maximum, in 0.60 intervals. For (b), the contour lines start at 0.50 and proceed to a 6.5 maximum in 1.0 intervals. For (c) the contour lines start at 0.50 and proceed to a 5.3 maximum in 0.8 intervals. Finally, for (d) the contours start at 0.25 and proceed to 1.66 in 0.28 intervals. To increase readability by highlighting peaks, power above the maximum minus 0.5 was truncated, except for (d) in which 0.3 was used to truncate the higher peaks. The time window step for (a) was 28 days, for (b) and (c) 27 days, and for (d) 25 days.

An important consideration in dynamic power spectra is how to determine the step to move the window through the time series. For the autocorrelation algorithm used in this study, which was

selected for its ability to ignore missing data, moving the running window at a time step other than the period of interest (or it's harmonics and subharmonics) will cause the power spectral density to show a periodicity of varying frequency. This effect is due to the loss of phase information in the autocorrelation algorithm employed here. An example of this can be seen in X_b of Figure 2, in which the 153-day period shows "islands" of power with a slope from the vertical. If the running window is stepped at 153 days, the contour diagram will show a single vertical island of power in the contour diagram. To reduce this effect, the running window was stepped in time at the number of days most near the rotational period that produced the maximum frequency stability. Hence the step sizes range from 25–28 days. However, there are a number of examples (some not shown here) in which no window step choice will straighten out a particular periodicity. In Figure 2, the weak periods between 16 to 18 days in S are such a case: the slope changes too much to be due to the spectral analysis. Other examples can be found near 27 days in $R(\mathrm{MgII_{c/w}})$ and $F_{10.7}$, in which there appears to be a gradual frequency modulation at sidebands of the 27-day periods. To better determine the frequency stability, an alternative technique should be employed.

A curious result of changing the step size of the running window to achieve maximum frequency stability is the resultant variation in the window step as a function of solar height. If we assume that the apparent synodic rotation rate corresponds to the running window step of maximum frequency stability, then the magnetic and photospheric sources S_{act} and S rotate at 25 days, the chromospheric $R(\mathrm{MgII_{c/w}})$ and $F_{10.7}$ at 27 days, and the coronal X_b at 28 days. This result is consistent with numerous earlier results (see for example El-Raey and Scherrer[11], Gilman[12], and Howard[13]).

The contour diagrams of the dynamic power spectra in Figure 2 demonstrate the quasiperiodic nature of solar variability. This is seen by observing that in Figure 2 many periodicities have amplitudes that are present for only a portion of the time series. For example, the roughly 300-day period in S almost completely disappears near solar minimum, and the 51-day period in X_b , $F_{10.7}$, and $R(\mathrm{MgII_{c/w}})$ is only present during solar maximum. Close inspection will show other instances. In a separate study by Pap *et al.*[14], it is also shown that there are dramatic differences in the power spectra of all solar indices determined during the ascending and descending portions of the solar cycle.

An interesting feature in Figure 2 is the wide range of periodicities in X_b from 25 to about 36 days, and to a lesser extent the 16 to 25-day periods. Because of the square waveform shape of an X–ray source caused by the rotation of the major sources across the visible disk in an optically thin solar atmosphere (see for example, Donnelly[15]), a broad fundamental frequency and many of its harmonics and subharmonics will appear in the power spectra. This effect of a non-sinusoidal waveform shape due to the rotation of a source, terrestrial viewing angle, and limb darkening effects can also clearly be seen in S and S_{act} , and to a lesser extent $F_{10.7}$. Since the rotational amplitude in $R(\mathrm{MgII_{c/w}})$ in more sinusoidal in its waveform shape due to the center-to-limb variation, the odd harmonics of the 27-day period are not visible in Figure 2. A second effect that may cause a broad range of periodicities around 36 days may be due to some as yet undetermined physical cause.

Another interesting feature in Figure 2 is the 150 to 155-day period that is dominant in X_b for the duration of the time series. This period is also strong in $F_{10.7}$ during the descending portion of the cycle, but is replaced by a 300-day period during solar minimum. Note that the 150 to

155-day period is only weakly present in S during solar maximum and nearly non-existent in $R(\mathrm{MgII}_{c/w})$. In contrast, consider the relatively simple dynamic spectra in $R(\mathrm{MgII}_{c/w})$: only the 27-day and 300 to 310-day periods dominate the contour diagram. Also note how $F_{10.7}$ show characteristics of both X_b and $R(\mathrm{MgII}_{c/w})$.

S produces ill-resolved power mostly around a 300-day period, with a broad range of relatively weak power from about 36 to 64 days, and from about 80 to 150 days. There are a number of stable periods very near 51 days, and to a lesser extent near 25 days. Actually, the power seems to appear in S at narrow sidebands of the 51 and 25-day periods, and the nearly vertical lines in the contour plots suggest constant frequency stability. Note that since power is calculated in Figure 2 as the percent of total power at a particular frequency, the result is that power near 51 and 25 days is enhanced with respect to the intermediate-term variations during solar minimum. Also recall sunspot blocking effects and faculae are competing effects on S , resulting in complicated power at sidebands of the 27-days rotational period, as discussed by Foukal and Lean[16]. The somewhat random longitudinal appearance of sunspot blocking effects and lack of persistence of these effects (typically less than two solar rotations), could also produce unusual periodicities in S .

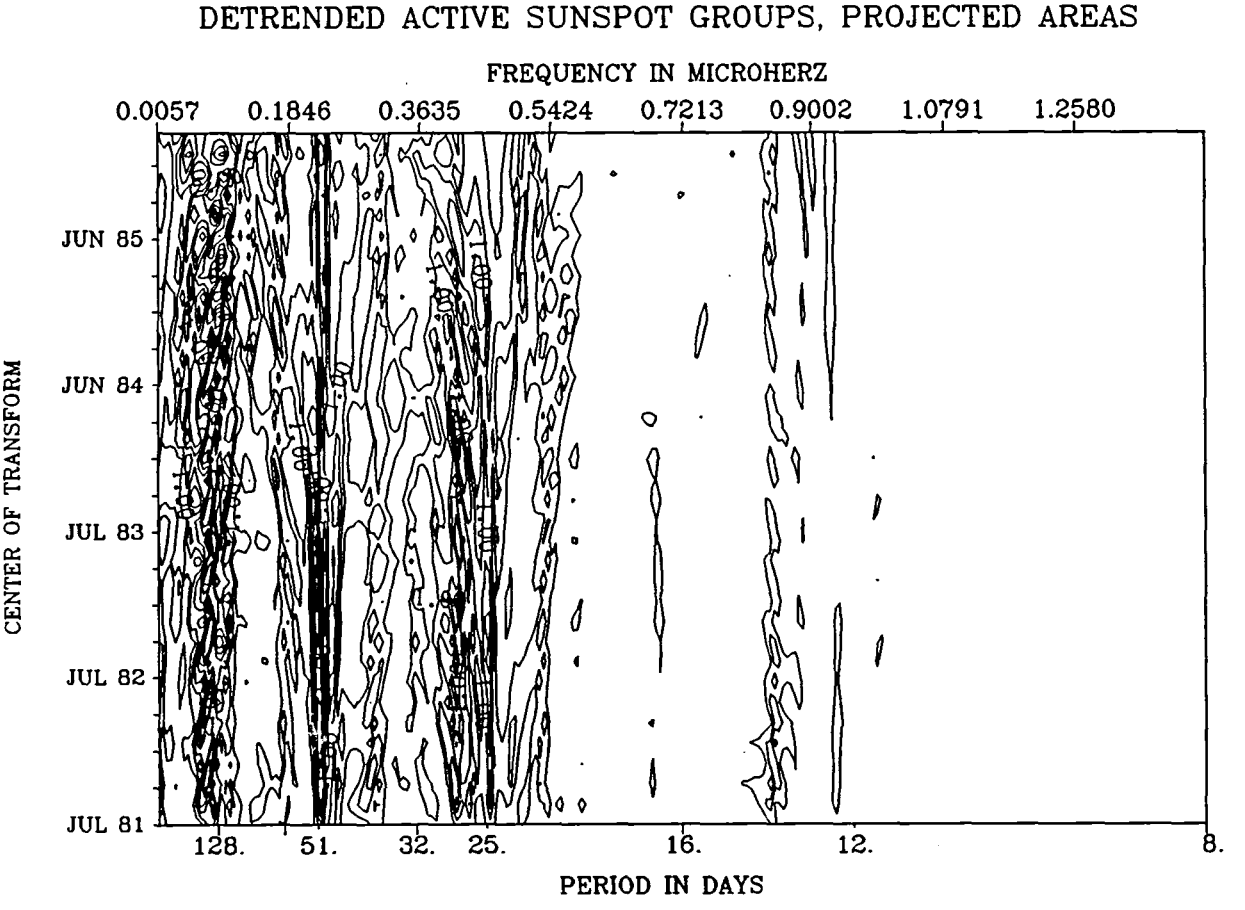

Figure 3. Enlarged dynamic power spectra of active sunspots *Sa* using a running 1024-day window, stepped by every 25 days, and enlarging the bottom scale to more clearly show shorter periods. Contours start at 0.50 and proceed to a maximum of 3.00 in 0.50 intervals, and power above 0.5 of the maximum was truncated.

In order to more closely examine the source of the 51-day period and it's harmonics, S_{act} is shown in Figure 3 for periods down to 8 days, and for a slightly longer time series than indicated in Figure 1. By using an active sunspot index, we are in effect looking down the magnetic field lines of emerging magnetic flux to deep sub-photospheric layers. Clearly, the 51-day period persists with the most power and stability for the duration of the time series. The 25-day period is strong, but weakens in power during solar minimum when only a few sunspots are formed. The 12.5-day period is present, but with weak amplitude. The unstable periodicities around 150 days slowly show more power near 300 days during solar minimum. Note the periods near 13.7 days: these are not harmonics of the 27-day period, but represent the fact that active regions tend to be distributed about 180 degrees in solar longitude, as suggested by Donnelly *et al.*.[17] It is important to note that a similar analysis of the projected area of passive sunspot groups (not shown here) yields a distinctly different dynamic power spectra: The majority of power can be found in passive sunspot periodicities around 27, 32–36, and 150-300 days. Clearly S_{act} and S demonstrate that emerging magnetic fields dominate photospheric time series measurements, and that a 51-day period of stable frequency is the fundamental period.

CONCLUSIONS

Power spectral density as a function of the solar cycle phase shows major differences between the solar source regions described here as photospheric, chromospheric, and coronal. There is compelling evidence to suggest the quasiperiodic nature of solar periodicities at solar rotation and active region evolution time scales. Remarkable is the stability in frequency of periodicities related to new emerging magnetic structures.

The period found in the data analyzed in this study that is most stationary in frequency and amplitude is the 51-day period in S_{act} and S . This is a most unexpected and unexplained result: When one considers that at any particular time some number of sunspots distributed in solar longitude and at various stages of evolution all exhibit roughly the same characteristics of amplitude and frequency, then one is inclined to at least suggest that some process is affecting all new sunspots in exactly the same fashion. Since the 51-day period has more power in S and S_{act} than short or intermediate periodicities, and because the 51-day period is sometimes present when 150-300 day periods are not, we know that it is not simply a sub-harmonic of solar rotation or a harmonic of intermediate-term periodicities. Part of the reason the 51-day period is so well resolved is because it lies in a portion of the frequency grid that is well isolated from the interfering effects of the adjacent 27-day and 150-day periods. If the 51-day period were intermittently present in the time series, then it's relative power would be severely diminished and it's spectral peak very broad in frequency, and this is not the case in the measurements except during solar minimum. While a number of authors have reported the 51-day period before, Bai[18] emphasized its importance in major flare occurrences, which are related to emerging magnetic structures.

The chromospheric observations seem to be dominated by an undetermined convective process on the order of 300 days modulating UV flux. The high-temperature portions of the corona are dominated by an approximately 150-day period, and emerging magnetic fields show equally strong periods at 51 and 150 days. Lean and Brueckner[19] discuss the characteristics of magnetic flux with associated with the 155-day periods, observing the period in sunspot blocking but not seeing it in plages. The dynamic spectral analysis in this study with respect to the 51-day period suggests that emerging magnetic flux has a major effect on photospheric flux, barely effects chromospheric

flux, and has a moderate effect on coronal flux at high temperatures (e.g., 3×10^6 °K).

Finally, the effectiveness of dynamic spectral analysis in describing solar variability sheds a new light on more traditional periodicity analysis techniques. The sun is far too complex of an oscillator to attempt to characterize it's variability with a single index or analysis technique. The fundamental assumption that needs to be challenged in many forms of statistical analysis of solar variability is the stationary presupposition: the mean, standard deviation, and autocorrelation of solar data often are not constant in time, and this may effect the interpretation of results derived from linear statistical techniques that assume stationarity.

ACKNOWLEDGEMENTS

We express our gratitude to Dr. R. C. Willson for providing the SMM/ACRIM data, Dr. D. Heath for providing and Nimbus-7 SBUV data, and Dr. W. Wagner for providing the GOES X-ray data. This research was supported by a grant of the NOAA/Sun-Climate Staff.

REFERENCES

1. Bouwer, S.D., "Intermediate-term epochs in solar soft X-ray emission", J. Geophys. Res., **88**, 7823–7830, 1983.
2. Donnelly, R. F., Heath, D. F., Lean, J. L., "Active-region evolution and solar-rotation variations in solar UV irradiance, total solar irradiance, and soft X rays", J. Geophys. Res., **82**, 10,318–10,324, 1982.
3. Donnelly, R. F., "Temporal trends of solar EUV and UV full-disk fluxes", Solar Phys., **109**, 37–58, 1987.
4. Bath, M., Spectral Analysis in Geophysics, p.125, Elsevier Sci., 1974.
5. Lean, J.L., and Repoff, T.P., "A statistical analysis of solar flux variations over time scales of solar rotation: 1978-1982", J. Geophys. Res., **92**, 5555–5563, 1987.
6. Smith, E.V.P., Gottlieb, D.M., "Solar flux and its variations", Space Science Reviews., **16**, 771–802, 1974.
7. Pap, J., "Variation of the solar constant during the solar cycle", Astrophys. Space Sci. **127**, 55, 1986.
8. Heath, D.F., Schlesinger, B.M., "The Mg 280-nm doublet as a monitor of changes in solar ultraviolet irradiance", J. Geophys. Res., **91**, 8672–8682, 1986.
9. Tobiska,W. K., Bouwer, S. D., "Intermediate-term variations of chromospheric and coronal solar flux during high solar cycle 21 activity", Geophys. Res. Lett., **8** , 779–782, 1989.
10. Wagner, W.J., "Observations of 1-8 Å solar X-ray variability during solar cycle 21", Paper 12.2.2, Helsinki COSPAR meeting, July 1988.
11. El-Raey, M., Scherrer, P.H., "Differential Rotation in the solar atmosphere inferred from optical, radio, and interplanetary data", Solar Phys., **26**, 15–20, 1972
12. Gilman, P.A., "Solar rotation", Annual Review of Astro. & Astro., **12** , 47–70, 1974.
13. Howard, R., "The rotation of the sun", Rev. Geophys.& Space Phy., **16**, 4, 721–732, 1978.
14. Pap, J, Tobiska, W.K., Bouwer, S.D., "Periodicities of solar irradiance and solar activity indices I", accepted by Solar Physics, Apr. 1990.
15. Donnelly, R.F., "Comparison of nonflare solar soft X ray flux with 10.7 cm flux", J. Geophys. Res., **87**, 6331–6334, 1982.
16. Foukal, P., Lean, J., "The influence of faculae on total solar irradiance and luminosity", Astrophys. J., **265**, 1056, 1983.
17. Donnelly, R. F., J.W. Harvey, D.F. Heath, T.P. Repoff, "Temporal characteristics of the Solar UV Flux and He I line at 1083 nm", J. Geophys. Res., **90**, 6267–6273, 1985.
18. Bai, T., "Periodicities of the flare occurance rate in solar cycle 19", Astrophys. J., **318**, L85-L91, 1987.